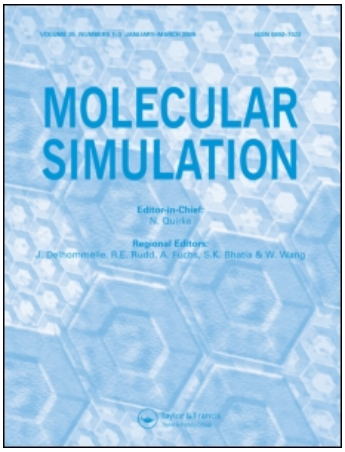

Molecular Simulation
Publication details, including instructions for authors and subscription information:
http://www.informaworld.com/smpp/title~content=t713644482

Diffusion enhancement in composites of nanotubes and porous structures

Simcha Srebnik[a]; Moshe Sheintuch[a]
[a] Department of Chemical Engineering, Technion-Israel Institute of Technology, Haifa, Israel

First published on: 21 September 2010

To cite this Article Srebnik, Simcha and Sheintuch, Moshe(2009) 'Diffusion enhancement in composites of nanotubes and porous structures', Molecular Simulation, 35: 1, 100 — 108, First published on: 21 September 2010 (iFirst)
To link to this Article: DOI: 10.1080/08927020802403858
URL: http://dx.doi.org/10.1080/08927020802403858

Molecular Simulation
Vol. 35, Nos. 1–2, January–February 2009, 100–108

Taylor & Francis
Taylor & Francis Group

Diffusion enhancement in composites of nanotubes and porous structures

Simcha Srebnik* and Moshe Sheintuch*

Department of Chemical Engineering, Technion–Israel Institute of Technology, Haifa, Israel

(*Received 11 May 2008; final version received 11 August 2008*)

Composites are often used to obtain enhanced material properties, including improved mechanical performance, enhanced conductivity, increased transport and other properties. Recent advances in carbon nanotube (CNT) composite porous materials suggest that CNTs may offer a greater advantage than conventional fillers, not only due to their extraordinary mechanical and electronic properties but also due to their smooth potential surface that allows for relatively high flux through the tubes. Using lattice Monte Carlo simulation, we study activated diffusion through various porous structures, and compare it with CNT composite materials. Flux enhancement is found to be substantial beyond the percolation threshold of nanotube aggregates, especially for relatively low-porosity structures. The simulation results are captured by a simple model that accounts for two contributions to the flux: diffusion within the percolating nanotube clusters and inside the porous substrate. Such porous structures may form better catalysts, membranes or molecular sieves where an increase in both surface area and flux is required.

Keywords: activated diffusion; nanotubes; simulation

1. Introduction

Porous materials are employed as catalysts, membranes, adsorbents and molecular sieves. Intensifying these processes implies having a larger surface area as well as acquiring high fluxes through these materials. These are, of course, contradicting constraints as a large surface area implies smaller pores that, in turn, imply lower diffusivity in the Knudsen or configurational diffusion regimes. This is especially true in the latter and largely ill-defined case where the forces between the walls and diffusing molecules are accounted for and the diffusion is activated. The availability of novel structures like carbon nanotubes (CNTs), which offer very small diffusion resistance due to their relative smooth potential surface [1], suggests that new composite structures, in which the CNTs are embedded within the porous ceramic or polymer material, may offer reduced resistance to diffusion. The purpose of this work is to study the activated diffusion dependence on the incorporation of CNTs to a porous substrate. We begin with a brief overview on nanocomposite materials, which have been shown to attain enhanced permeation properties, as a benchmark for comparing our study on CNT composites.

Polymer nanocomposites have received vast attention since the discovery of the extraordinarily enhanced properties of polymer–clay hybrid materials [2,3], which exhibit substantial improvement in strength, modulus and distortion temperature when compared with the pure polymer [4], in addition to substantial enhancement of permeation properties when nanosized particles are used. In particular, it has been found that the addition of 10–30 wt% of controlled nanosized particles can increase small penetrant permeation by up to an order of magnitude [5,6]. The anomalous behaviour observed for nanosized particles compared with the same loading of larger filler particles (which *reduce* diffusivity with loading) is believed to be associated with the greater specific interfacial area of the nanoparticle composite. These findings incited extensive research using computational modelling methods [7], focusing largely on the structural and mechanical properties of polymer–clay composites.

Nanotube reinforcement of polymer and ceramic composites have been recently considered due to their greatly enhanced electrical conductivity as well as mechanical properties [8]. The enhanced electrical properties have been analysed in the context of percolation theory of fibrous materials with long aspect ratios [9–11]. Since the primary charge-transport mechanism in nanotube-reinforced composites is electron tunnelling [12,13], the nanotubes need to be in close vicinity but are not required to be in physical contact. Thus, the percolation-like behaviour can be attributed to the formation of an effective percolating cluster, in which the nearest neighbour particles are within a certain tunnelling range from one another [10]. While this feature suggests that electrical percolation may not be synonymous with geometric percolation [14], for diffusion within hollow fillers, a similar concept of 'percolation distance' is needed, as we further discuss in the following section.

*Corresponding authors. Email: simchas@technion.ac.il; cermsll@technion.ac.il

ISSN 0892-7022 print/ISSN 1029-0435 online

DOI: 10.1080/08927020802403858
http://www.informaworld.com

Another mode to control the porous structure of a material is by templating, in which pores of predetermined size or chemical affinity within a material [15–17] are created. This technique has mostly been studied for applications requiring molecular separation based on size and shape. In this approach, a porous material, such as a gel, is formed in the presence of 'template' molecules. The templates are usually removed after gelation is completed, leaving behind pores that correspond in shape and size (and functionality in the case of molecular imprinting) to the template molecules. In addition to improved size selectivity in molecular sieving, the main benefit of templating is the reduction of weight of the material with only a modest decrease in strength [17]. The effect of templating on diffusivity has been studied using molecular dynamics simulations [18] where it was observed that for a given porosity, non-activated diffusivity of a fluid within a material prepared without a template is higher than in any other templated material. That is, while the overall porosity of the templated material is higher, the lower effective porosity of the walls surrounding the templated pores leads to an overall reduction in the diffusivity. This is in contrast to the enhanced diffusivity observed in general with increasing porosity, as well as the enhanced diffusivity seen with nanoparticle composites [19–25]. We will return to this point in our study of CNT composites.

In addition to the porous structure, the diffusivity may be strongly influenced by interactions of the diffusing particles with the solid walls, as has been shown in simulations of activated diffusion in zeolites [26,27] and disordered porous materials [28,29]. Yashonath and Santikary [26] showed that, in some cases, smaller windows between cages may lead to enhanced cage hopping, a result that is counter-intuitive to geometrical considerations only. Further calculations revealed that the smaller openings lacked activation energy, and thus allowed for enhanced hopping. However, these findings depend on the size of the diffusing particle [27]. In the case of disordered materials, the overall diffusivity through the material is known to decrease with increasing attractive particle–wall interaction strengths [28,29]. It was further shown that the effective diffusivity can be approximated from the knowledge of the energy barriers associated with every pore and the pore size distribution, which, for a random structured object, can be predicted analytically [28].

In this work, we analyze activated diffusion through CNT composite porous materials. In light of the above studies, CNTs may be regarded as both fillers (or obstacles to diffusion of particles outside the CNTs) and 'templated' pores (for particles diffusing inside the CNTs). The effect of CNTs on diffusivity is compared with that in analogous templated materials and in nanoparticle composites. An approximate analytical solution is presented for activated diffusion through CNT composites, accounting for the relative contributions of particle diffusion inside the CNT cluster, which is apparently percolating due to tunnelling, and within the porous material.

2. Model

Cluster–cluster aggregation (CCA) [30] is used to simulate the formation of porous materials in the presence of tubular fillers (model CNTs) or templates on a cubic lattice, of size L, with periodic boundaries. In our model, the filler occupies a number l_t of consecutive lattice sites, each of size σ (typically, one site). Initially, a chosen number of fillers is placed in a random location and with a random orientation on the three-dimensional lattice (horizontal or vertical) according to a prescribed volume fraction, ϕ. Then, a given fraction $\phi_w = 1 - \varepsilon$ (where ε is the porosity of the material in the absence of the fillers) of lattice sites is randomly filled with 'wall' building blocks, each occupying a single lattice site. Aggregation follows through a series of trial moves, in which a random particle or cluster is selected and a move is attempted in a random direction. If there is no overlap between the new positions of the particles making up the cluster and other particles on the lattice, the move is accepted, and cluster lists are updated to account for the possibility of newly formed contacts between neighbouring particles in the new configuration.

Diffusion within the composite is simulated on a fine grid (size 0.25σ) embedded in the original cubic lattice. At the beginning of the diffusion simulation, the potential that a diffusing particle of size σ would feel at each location on the finer grid is calculated and stored, so that diffusion is simulated on a potential map of the composite material. Interactions between the diffusing particles are neglected in our study (though particle loading has been shown to affect particle path [31,32]) while interactions between particles and walls are assumed to be of the Lennard-Jones type, according to

$$U = \kappa\left[\left(\frac{\sigma}{r}\right)^{12} - \left(\frac{\sigma}{r}\right)^{6}\right], \tag{1}$$

where U is the potential energy, r the distance between the centre of mass of the two interacting particles, and κ and σ the Lennard-Jones parameters corresponding to the effective interaction strength and molecular size, respectively. The cut-off radius for the potential is fixed at $r_c = 2\sigma$. The nanotubes are assumed to have infinitely thin impenetrable walls, with a uniform potential inside the tube, as shown in Figure 1. The inner layer of the CNT walls is taken to be reflective [33], as described below.

In each diffusion iteration, a random direction for movement is chosen, with a maximum step length given by $r_{max}(p) = -\mu \ln p$, where μ determines the mean free

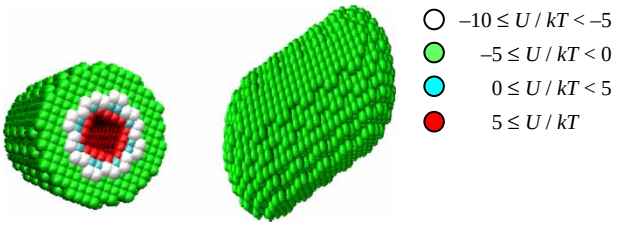

Figure 1. Potential energy around the nanotube for $\kappa/kT = 10$ and $l_t = 5$.

path of the diffusing particle and p is a random number on the interval [0,1). In vacuum, when μ is set to a unit step length, the measured average mean free path is $\mu_0 = 0.88\sigma$. However, in the presence of particles (wall or filler), the actual step length traversed is determined by the total energy of the diffusing particle at the beginning of the move, and the potential energy along the path in the direction of the move [28]. That is, prior to movement, the particle is assigned a random kinetic energy calculated from the Boltzmann distribution according to

$$f(E) \propto e^{-E/kT}, \tag{2}$$

where $f(E)$ is the probability of having energy E at the prescribed temperature of the simulations. The total energy of the particle prior to movement is then given by the sum of the kinetic energy E and potential energy U at its current site. Then, the particle begins to move along its chosen path, and continues to move as long as its total energy $(E + U)$ is higher than the potential energy encountered along the path. Therefore, since a particle may reach a potential energy barrier before it completes a path of length $|r_{max}|$, the actual mean free path is usually less than μ_0.

Diffusion within the CNTs, however, is not hindered or activated due to their smooth potential surface [1,33]. Accordingly, the interior wall of the CNTs is modelled as reflective in the direction of the long axis of the CNT [33]. That is, for a tube whose axis is in the z-direction, a particle travelling along a vector (dx,dy,dz) will be reflected as it hits the wall and will continue its path along the vector ($-$ dx, $-$ dy,dz).

The effective particle diffusivity is then calculated in two ways: through average diffusivity over a fixed period of time (referred to as Einstein diffusion) and through the distribution of exit times of the particles needed to cross a fixed length of the material in the z-axis (Fick's second law of diffusion). Due to computational limitations, each diffusion simulation is carried out on one or several realisations of the porous solid. Clearly, proper statistical sampling should involve averages over large number of structures. However, the use of a relatively large lattice and the clear trends observed with changing ε or ϕ, which represent different realisations of the solid, make the results statistically representative.

In the Einstein experiment, 1000 particles are randomly distributed anywhere in the finer grid, with a probability proportional to its Boltzmann factor, $e^{-\beta u_s}$, where u_s is the potential at that site. Accordingly, if the initial trial position of a particle is at a low-energy site, it is always accepted, while a trial position at a high-energy site will be accepted according to its Boltzmann factor. This approach provides an initial distribution that is expected to be similar to an equilibrium distribution. The particles are then allowed to diffuse over 10^6 iterations, and the average diffusivity is calculated over the last 10^4 iterations. This period was found to be sufficient to bring the system to equilibrium for the range of parameters studied. The average Einstein diffusivity is obtained from

$$D = \frac{1}{6N_d\Delta t}\sum_{j=1}^{N_d}\sum_{i=t_1}^{t_2}(r_{j,i} - r_{j,i-1})^2, \tag{3}$$

where N_d is the number of diffusing particles, $r_{j,i}$ the position of particle j at time i, t_1 and t_2 the initial and final times for calculating the average and $\Delta t = t_2 - t_1$.

Diffusivity, according to Fick, is calculated from the exit time distribution of particles, initially distributed at the top layer of the finer grid. The particles are then allowed to traverse a distance $|L_z|$ of the matrix in the z-axis, with no requirement of a fixed distance in the x- and y-axes. In this case, the probability $P(L;t)$ of a particle to displace a distance L in the z-direction at a given time, t, may be calculated from [28]

$$\begin{aligned} P(L;t) &= \frac{1}{(4\pi D_F t)^{3/2}}\int_0^{L_x} dx \int_0^{L_y} dy \exp\left(-\frac{x^2+y^2+L^2}{4D_F t}\right) \\ &= \frac{C}{(D_F t)^{1/2}}\exp\left(-\frac{L^2}{4D_F t}\right)\operatorname{erf}\left(\frac{L_x}{(4D_F t)^{1/2}}\right) \\ &\quad \operatorname{erf}\left(\frac{L_y}{(4D_F t)^{1/2}}\right), \end{aligned} \tag{4}$$

where D_F is the diffusion coefficient obtained from the distribution of exit times, and L_x and L_y are the maximal observed absolute displacement of the particle in the x- and y-axes, respectively. The function $P(L;t)$ has a maximum defined by D_F for a given L. D_F is determined by adjusting the maximum of the analytical distribution to that of the simulated results and minimising the mean square error [28]. We note that while a proper theoretical treatment of activated diffusion in the composite should involve first-passage time approach [34], Equation (4) provides a reasonable fit for the average diffusivity in our simulated system.

3. Results and discussion

Incorporation of CNT fillers is expected to have two main effects. On the one hand, the CNTs will inhibit the diffusion flux through the porous material, as the effective void fraction is reduced (keeping overall void fraction constant). On the other hand, flux through the CNTs offers reduced resistance, at least once apparent percolation of the CNTs is obtained. To quantify these effects, we need to determine first the percolation threshold of CNT clusters and its dependence on nanotube length. We will use this information below when we develop an approximate expression for the overall diffusivity.

3.1 Percolation threshold

It has been demonstrated, both experimentally [19–22] and theoretically [23–25], that the shape and size of the filler has a significant effect on the percolation threshold of a composite (e.g. the formation of pathways along the outside walls of the fillers), and thus should influence penetrant diffusivity [35]. We define the percolation threshold for diffusion through the nanotube fillers by the CNT volume fraction, ϕ_p, beyond which a percolating cluster of CNTs exists. The threshold is calculated by first accounting for the different CNT clusters, and then checking whether at least one cluster percolates in all three dimensions. However, since two CNTs will seldomly perfectly align end to end, we need to allow for 'soft percolation' by allowing small separation of two NTs. Under this definition, two nanotubes are said to belong to the same 'diffusion' cluster if their ends are within the distance σ, as illustrated in Figure 2(a). Note that if an open end of a nanotube faces the edge of another nanotube, then they are not considered to belong to the same cluster, since that configuration presents a dead end for diffusion (Figure 2(b)). Note also that this definition will not affect the numerical diffusion simulation, but will affect the following approximation.

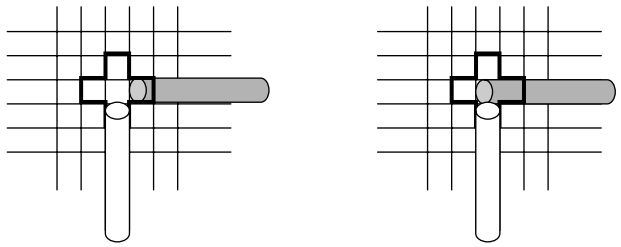

Figure 2. Two-dimensional representation of the definition for diffusion percolation cluster of nanotubes. Nanotubes are said to be part of the same diffusion percolation cluster of the white tube if their ends are within the distance σ of one of its ends (outlined area), but do not block it. The scenario on the left presents two CNTs belonging to the same cluster, but the one on the right does not.

The percolation threshold ϕ_p for nanotubes, defined in this manner, grows linearly with tube length, l_t (Figure 3), so that the concentration of the tube ends at percolation remains essentially constant, independent of l_t. The linear growth might be anticipated from the following argument. Consider the bond percolation problem for sticks (or bonds) of length l_t placed on a cubic lattice with bond size l_t. The percolation in this case is given by ϕ_b/l_t where ϕ_b is the known bond percolation threshold for $l_t = 1$. However, the actual grid is made of bonds of size l_t and we should consider l_t^2 such grids, each a duplicate spatially shifted version of the original grid. We ignore jumps from one grid to another. Thus, we obtain

$$\phi_p \propto \left(\frac{\phi_b}{l_t}\right) l_t^2 \propto l_t. \tag{5}$$

In Figure 4, we compare the pore percolation threshold of a composite upon addition of nanotube fillers (concentrating on $l_t = 5\sigma$). We plot the effective porosity of the composite at the pore percolation threshold as a function of filler (rod or nanotube) concentration. In the case of rod fillers, the effective porosity is simply the volume fraction of voids in the composite $\varepsilon_{\text{eff}} = \varepsilon - \phi$. Rods reduce the pore percolation of the composite only slightly, from $p_c = 0.32$ for a pure substrate to 0.28 for a composite with 50% filler due to the presence of somewhat larger pores with increasing ϕ. This, in turn, leads to somewhat higher diffusion rates (Figure 7(b)). In the case of the nanotubes, we define the effective porosity as

$$\varepsilon_{\text{eff}} = \varepsilon - \left(\frac{4l_t\sigma}{4l_t\sigma + 2\sigma^2}\right)\phi, \tag{6}$$

since percolation cannot occur through the sides of the tube (whose area is $4l_t\sigma$), but only through the two ends

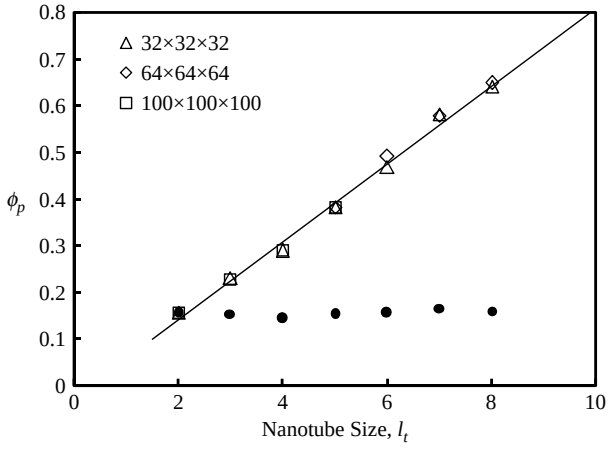

Figure 3. Percolation threshold as a function nanotube size for various lattice sizes for (white symbols). Black diamonds show the change in the concentration of nanotube ends as a function of tube size.

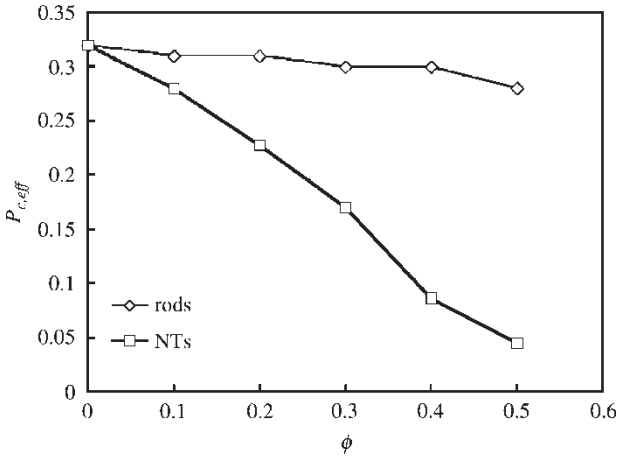

Figure 4. $p_{c,\mathrm{eff}}$ as a function of volume fraction of rod (diamonds) and nanotube (squares) fillers.

of the tubes (area $2\sigma^2$). Note that for our applications (with $l_t = 5$, $\sigma = 1$), $\varepsilon_{\mathrm{eff}} = \varepsilon - 20\sigma/22$, which is not significantly different from the $\varepsilon_{\mathrm{eff}} = \varepsilon - \phi$ used for rods. We recorded the effective percolation threshold using this definition: Figure 4 shows that the addition of the nanotubes enhances pore percolation significantly, even at relatively low CNT concentrations. Since for long CNTs (large l_t) $\varepsilon_{\mathrm{eff}} \approx \varepsilon - \phi$, the observed decrease in p_c is clearly due to the CNT channels connecting pores that would otherwise remain isolated, and hence should lead to significantly enhanced penetrant diffusivity.

3.2 Estimating the diffusivity

Several examples for obtaining the diffusivity using the exit time method (Equation (4)) are shown in Figure 5. The inset of Figure 5 shows the increase in the squared displacement with time, which is used to approximate D from Equation (3). The values of D obtained from Equation (4) (indicated in the figure) for the most part compare very well with those obtained from the much less computationally demanding method of the Einstein diffusion experiment that corresponds to the average diffusivity through the composite at thermodynamic equilibrium. Interestingly, if we follow the average squared distance travelled with time for a composite with $\phi \cong \phi_p$ and ε somewhat greater than ϕ (Figure 5(c)), we observe a clear transition from faster ($D = 0.01$) to slower diffusion ($D = 0.0008$). Nonetheless, D obtained from Equation (3) corresponds very well to D approximated from Equation (4) for sufficiently long times, and therefore our results below present the average diffusivity, as measured by the Einstein diffusion experiment. This approximation is therefore correct for solids whose cross section is much larger than the average length of the CNTs.

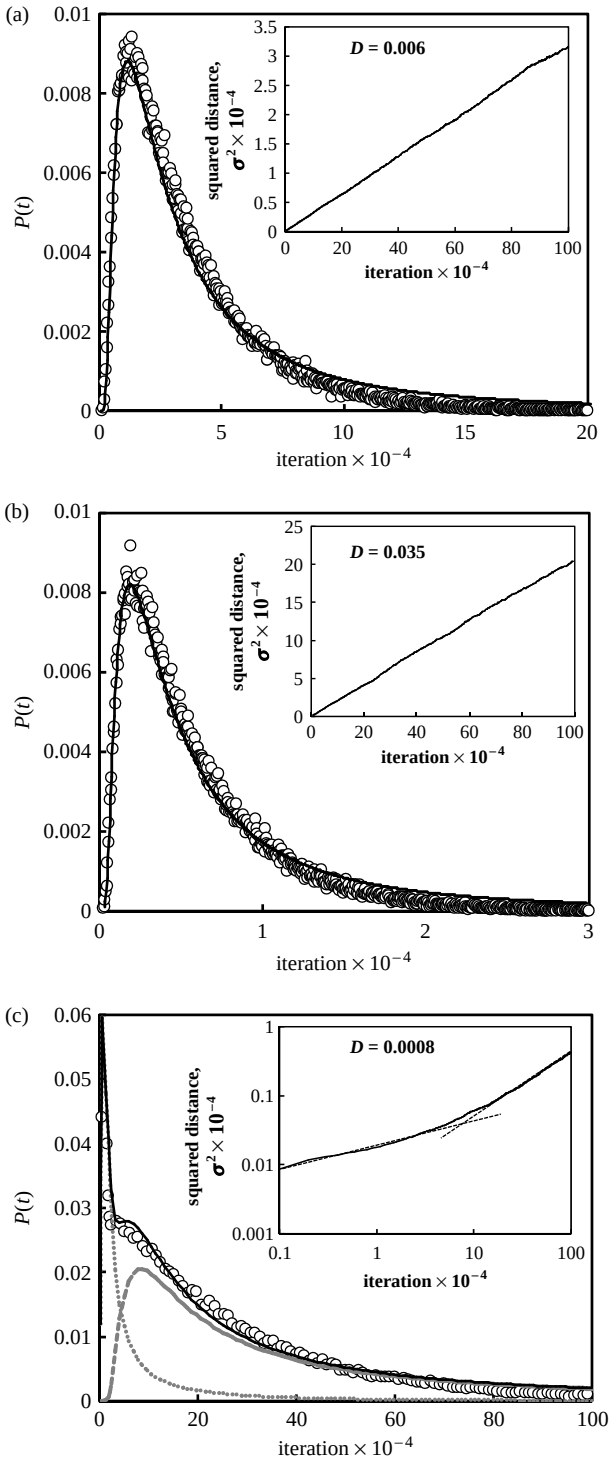

Figure 5. Diffusivity from exit times (symbols show simulation results, curve show prediction from Equation (4)) for (a) $\varepsilon = 0.6$, $\phi = 0.0$. (b) $\varepsilon = 0.6$, $\phi = 0.6$ and (c) $\varepsilon = 0.6$, $\phi = 0.5$ ($D = 0.01$, dotted grey curve; $D = 0.0008$, dashed grey curve). Inset shows the squared end-to-end distance with time obtained from the corresponding Einstein diffusion experiments, with the calculated diffusivity indicated in bold letters.

The diffusivity exhibits a local minimum with increasing volume fraction of nanotubes or with increasing substrate fraction (Figure 6). This effect follows from the two contradicting effects described above: incorporation of CNTs leads to more narrow passages and consequently smaller diffusivity of particles undergoing weak LJ interactions with the solid, but the diffusivity through the CNT is not activated and becomes stronger beyond percolation. This non-monotonic behaviour is not observed for other porous structures studied, and we will return to it in our analytical development below. We note that similar behaviour was predicted for diffusion in the cells [36].

To understand the various contributions, we compare the diffusivity of different composite schemes: CNTs, rods or blocked CNT, and templated material where the CNTs are replaced by a simple straight pore of the same size but in which diffusion is activated (Figure 7(a)). For the same concentration of the filler and substrate, the CNTs do not appear to provide any benefit when compared with the other two methods, except at very high CNT concentration. We will later explore, therefore, whether CNT incorporation will eventually pay off at high f. Nonetheless, when D is plotted against the effective porosity defined in Equation (6) (Figure 7(b)), CNT composites show significant improvement in flux over other materials, even at small values of ϕ. Note that in our study the increase in D with ϕ observe in the case of rods (Figure 1) is likely due to the presence of larger pores in the solid and not due to the presence of high-permeability pathways near the fillers [6,37].

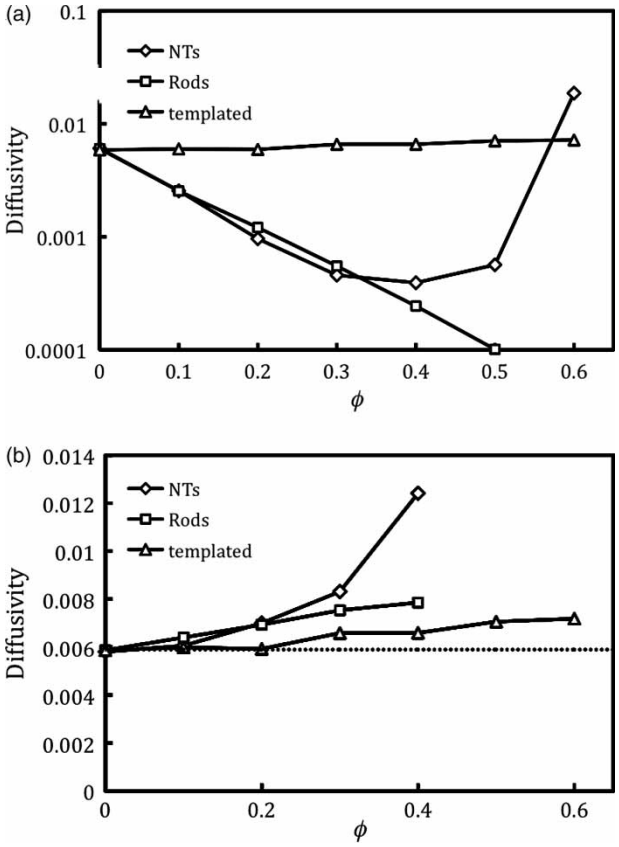

Figure 7. (a) Comparing diffusivity for various composites with $\varepsilon = 0.6$, rods (squares), CNTs (diamonds) and templated substrate (triangles). (b) Same as (a) but keeping the effective substrate porosity at $\varepsilon_{\text{eff}} = 0.6$, as calculated from Equation (6) (dashed line shows diffusivity through non-templated solid with $\varepsilon = 0.6$).

3.3 Analytical approximations

To obtain a better understanding of the contribution of the two diffusion pathways in the CNT composite towards the observed non-monotonic behaviour in Figure 6, we derive an approximate analytical prediction, which can be used later for structure optimisation. We assume that the two phases are distributed randomly within a cube of size $L^3 = (N\sigma)^3$. We will view the composite as a combination of two resistances in parallel: the porous material, which is described by a simple site percolation model, and by a cluster of CNTs, which is continuous beyond the CNT percolation threshold, f_p. For a highly activated diffusion (high κ), in the site percolation cluster, we can use the results of Srebnik et al. [28] where we showed that the effective diffusivity can be predicted from the knowledge of pore size distribution and the energetic barrier dependence on each site. As might be anticipated [28], for high κ the diffusivity is greatly reduced below CNT percolation due to low-energy traps in the composite, and D is regained only when ϕ approaches ε (results not shown). For a range of high porosities, the dependence of the contribution to diffusivity in the pores, D_ε, can be described by $D_\varepsilon = A_\varepsilon \varepsilon e^{-K(1-\varepsilon)}/\tau_\varepsilon$, where τ_ε is the tortuosity associated with this structure where for large τ_ε we commonly write $\tau_e = 1\varepsilon$ [38] and K is a constant. Placing rods in the

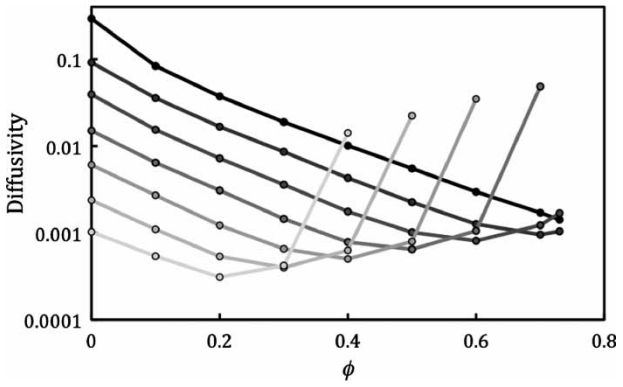

Figure 6. Effective diffusivity for various porosities as a function of nanotube concentration. Curves correspond to the following values of substrate porosity, from top to bottom: $\varepsilon = 1.0$, 0.9, 0.8, 0.7, 0.6, 0.5 and 0.4.

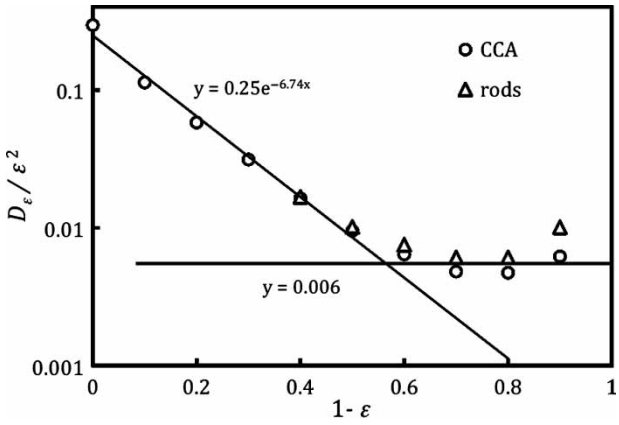

Figure 8. $D_\varepsilon/\varepsilon^2$ as a function of $1 - \varepsilon_{\text{eff}}$ in the absence of fillers ($\varepsilon_{\text{eff}} = \varepsilon$, circles) and for rod fillers (triangles).

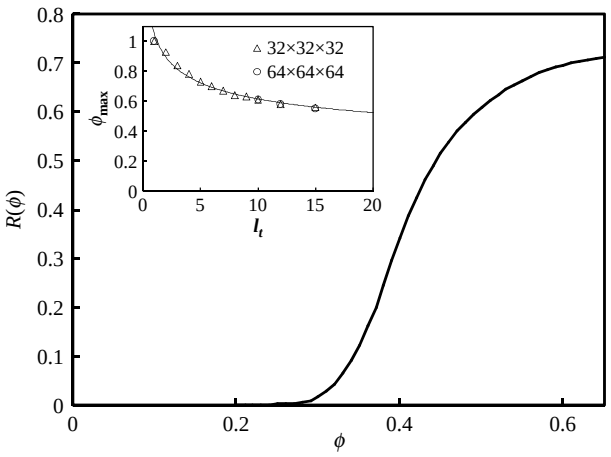

Figure 9. Probability of NT belonging to an infinite cluster as a function of normalised CNT concentration.

structure will cause the effective porosity of the solid to decline like $\varepsilon_{\text{eff}} = \varepsilon - \phi$, with an exponential decline of D_ε with ϕ, in agreement with simulations (Figure 7(a)). The parameters A_ε and K can be easily extracted from a plot of $D_\varepsilon\varepsilon^2$ (Figure 8) obtaining 0.25 and 6.7, respectively.

The contribution of the CNT clusters is evident beyond the percolation threshold. The probability of belonging to the largest cluster that connects both sides of the composite, $R(\phi)$, grows fast (Figure 9), but does not approach unity since the maximal concentration of CNTs is less than unity for $l_t > 1$ (see the inset of Figure 9), and hence cluster connectivity is limited. (While finite clusters contribute to diffusion for $\phi - \phi_p < 0$, this effect appears to be small, as evident from Figure 6 and is ignored in the following development.) We can view the big (infinite) cluster as a bond percolation cluster with units of size $l_t\sigma$ and a probability of finding a bond at any position is $\phi R(\phi)$, since the total numbers of CNTs is ϕL^3, of which $R(\phi)$ are part of the infinite cluster. The diffusivity within each CNT is D and the contribution of the cluster to the total diffusivity is $D_0\phi R(\phi)/\tau_\phi$, where τ_p is the tortuosity associated with this structure. The overall diffusivity due to both contributions is then

$$D = D_\varepsilon(\varepsilon - \phi)/\tau_\varepsilon + D_0\phi R(\phi)/\tau_\phi$$
$$\cong A_\varepsilon e^{-K(1-\varepsilon+\phi)}(\varepsilon - \phi)^2 + D_0[\phi R(\phi)]^2. \qquad (7)$$

When ϕ approaches ε, the probability that the open end of a tube is occupied by either a particle or another tube is high, and passage through the tube is likely to be blocked. Hence, if that tube belongs to the infinite cluster, then $R(\phi)$ is effectively shifted to higher values of ϕ, with $\phi_{\text{eff}} = \phi(\varepsilon - \phi)$. However, the use of spherical interactions centred at the sites of a cubic lattice combined with our model of CNTs with impenetrable walls of zero thickness, allows for non-negligible 'tunnelling' in such configurations (diffusion through the low-energy corners of the cubic sites). Thus, the effective CNT concentration at percolation is approximated as

$$\phi_{\text{eff}} = \phi\left[(\varepsilon - \phi) + \phi\left(\frac{1}{5} + \frac{4}{5}p_t\right)\right],$$

where the first term I the probability to find the site vacant and the second one represents the probability to find a NT at that site; in that case p_t accounts for the finite diffusivity across apparently blocked tubes. The allowed passage between seemingly blocked tubes presumably occurs in real systems due to non-ideal packing.

$R(\phi)$ in Equation (7) is calculated at $\phi = \phi_{\text{eff}}$. A comparison between the theoretical prediction and the simulation results shows a reasonable fit across the values of ϕ and ε, with $p_t = 0.5$ (Figure 10(a)). Note that this is the only fitted parameter in the model. The incorporation of CNT enhances the diffusivity at high ϕ and low ε. This is evident from the $\varepsilon = 0.5, 0.7$ curves. This effect will be stronger as the diffusion activation barrier increases: in Figure 10(b), we show the analytical prediction for highly activated diffusion. Clearly, for moderately to highly activated diffusion (large κ), CNT composites exhibit significantly better performance at lower values of ϕ.

4. Concluding remarks

While we have characterised the various effects on diffusion in a composite made by the incorporation of CNTs into a porous structure, and were able to adequately predict the behaviour, we wish now to consider the engineering question: will such an effort lead to higher fluxes in a catalyst or better size separation in a membrane? One piece of information missing in the analysis is the mechanical properties of the structure. It is safe to assume that a higher solid fraction will make

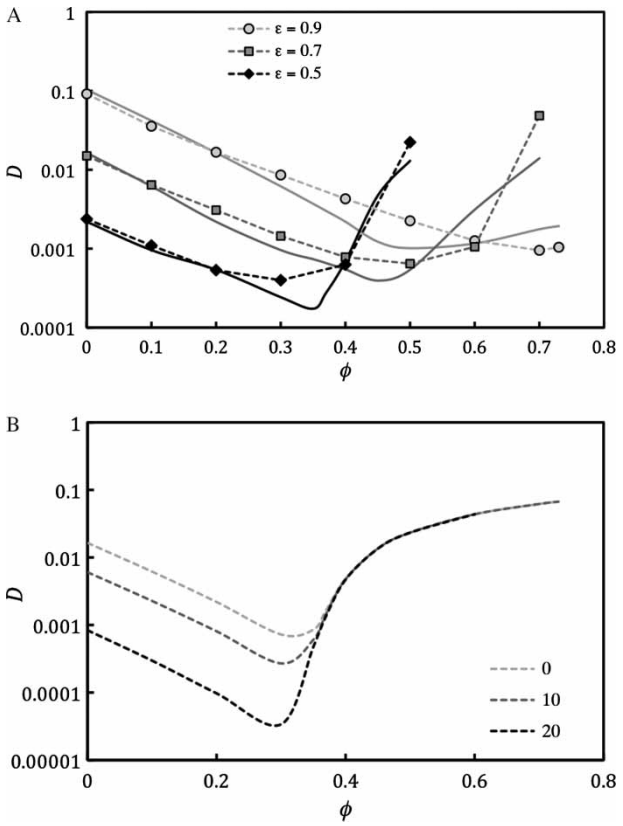

Figure 10. Diffusivity as a function of CNT concentration (a) as predicted from the simulations (dashed curves) and theory (solid curves) for various values of ε, for $\kappa = 4$, and (b) as predicted from theory for various values of κ (note that $\kappa = 4\varepsilon_{LJ}$, where ε_{LJ} is the commonly defined Lennard-Jones interaction parameter).

the composite more durable. This implies low porosity and these are the conditions under which the incorporation of CNTs may be advantageous. We should compare therefore two structures, one with porous material only and another with the largest fraction of CNTs possible. This fraction is limited only by the geometric constraint of incorporating nanotubes of a particular length in a random orientation within the composite (see the inset of Figure 9). This comparison corresponds to the left ($\phi = 0$) and right point of each curve in Figure 6, respectively. It is evident that the ratio of diffusivities between these two points goes through a maximum, at $\phi = 0.6$, at which there is more than a threefold increase in flux. These conditions, therefore, hold the potential for a 'durable and high flux materials'. The results, however, are very sensitive to the 'tunnelling' possibility from one CNT to another. Prior to experimental realisation of this idea, we should consider more carefully the CNT model and replace it with one of a finite wall thickness and a more accurate potential representation. This will lead, of course, to smaller samples or longer computations.

References

[1] A.I. Skoulidas, D.M. Ackerman, J.K. Johnson, and D.S. Sholl, *Rapid transport of gases in carbon nanotubes*, Phys. Rev. Lett. 89(18) (2002), p. 185901.

[2] A. Usuki, Y. Kojima, M. Kawasumi, A. Okada, Y. Fukushima, T. Kurauchi, and O. Kamigaito, *Synthesis of nylon 6-clay hybrid*, J. Mater. Res. 8(5) (1993), pp. 1179–1184.

[3] Y. Kojima, A. Usuki, M. Kawasumi, A. Okada, Y. Fukushima, T. Kurauchi, and O. Kamigaito, *Mechanical-properties of nylon 6-clay hybrid*, J. Mater. Res. 8(5) (1993), pp. 1185–1189.

[4] C.E. Powell and G.W. Beall, *Physical properties of polymer/clay nanocomposites*, Curr. Opin. Solid State Mater. Sci. 10(2) (2006), pp. 73–80.

[5] J.Y. Zhong, W.Y. Wen, and A.A. Jones, *Enhancement of diffusion in a high-permeability polymer by the addition of nanoparticles*, Macromolecules 36(17) (2003), pp. 6430–6432.

[6] T.C. Merkel, B.D. Freeman, R.J. Spontak, Z. He, I. Pinnau, P. Meakin, and A.J. Hill, *Ultrapermeable, reverse-selective nanocomposite membranes*, Science 296(5567) (2002), pp. 519–522.

[7] Q.H. Zeng, A.B. Yu, and G.Q. Lu, *Multiscale modeling and simulation of polymer nanocomposites*, Progr. Polym. Sci. 33(2) (2008), pp. 191–269.

[8] M. Moniruzzaman and K.I. Winey, *Polymer nanocomposites containing carbon nanotubes*, Macromolecules 39(16) (2006), pp. 5194–5205.

[9] J. Li, Z.B. Zhang and S.L. Zhang, *Percolation in random networks of heterogeneous nanotubes*, Appl. Phys. Lett. 91(25) (2007), pp. 253127–253500.

[10] L. Berhan and A.M. Sastry, *Modeling percolation in high-aspect-ratio fiber systems I. Soft-core versus hard-core models*, Phys. Rev. E 75(4) (2007), p. 041121.

[11] Z. Neda, R. Florian, and Y. Brechet, *Reconsideration of continuum percolation of isotropically oriented sticks in three dimensions*, Phys. Rev. E 59(3) (1999), pp. 3717–3719.

[12] F.M. Du, R.C. Scogna, W. Zhou, S. Brand, J.E. Fischer, and K.I. Winey, *Nanotube networks in polymer nanocomposites: Rheology and electrical conductivity*, Macromolecules 37(24) (2004), pp. 9048–9055.

[13] J.M. Benoit, B. Corraze, and O. Chauvet, *Localization Coulomb interactions, and electrical heating in single-wall carbon nanotubes/polymer composites*, Phys. Rev. B 65(24) (2002), p. 241405.

[14] M. Avellaneda and S. Torquato, *Rigorous link between fluid permeability, electrical-conductivity, and relaxation-times for transport in porous-media*, Phys. Fluids A Fluid Dyn. 3(11) (1991), pp. 2529–2540.

[15] P.G. de Gennes, *Possibilites allowed by polymer reticulation in presence of a liquid crystal*, Phys. Lett. A A28(11) (1969), p. 725.

[16] R.L. Rill, B.R. Locke, Y.J. Liu, J. Dharia, and D. VanWinkle, *Protein electrophoresis in polyacrylamide gels with templated pores*, Electrophoresis 17(8) (1996), pp. 1304–1312.

[17] R.L. Rill, D.H. Van Winkle, and B.R. Locke, *Templated pores in hydrogels for improved size selectivity in gel permeation chromatography*, Anal. Chem. 70(13) (1998), pp. 2433–2438.

[18] H. Dominguez and M. Rivera, *Studies of porosity and diffusion coefficient in porous matrices by computer simulations*, Mol. Phys. 100(24) (2002), pp. 3829–3838.

[19] M.L. Clingerman, E.H. Weber, J.A. King, and K.H. Schulz, *Synergistic effects of carbon fillers in electrically conductive nylon 6,6 and polycarbonate based resins*, Polym. Compos. 23(5) (2002), pp. 911–924.

[20] T. Ota, M. Fukushima, Y. Ishigure, H. Unuma, M. Takahashi, Y. Hikichi, and H. Suzuki, *Control of percolation curve by filler particle shape in Cu-SBR composites*, J. Mater. Sci. Lett. 16(14) (1997), pp. 1182–1183.

[21] H.S. Gokturk, T.J. Fiske, and D.M. Kalyon, *Effects of particle-shape and size distributions on the electrical and magnetic-properties of nickel/polyethylene composites*, J. Appl. Polym. Sci. 50(11) (1993), pp. 1891–1901.

[22] M.L. Clingerman, E.H. Weber, J.A. King, and K.H. Schulz, *Development of an additive equation for predicting the electrical*

conductivity of carbon-filled composites, J. Appl. Polym. Sci. 88(9) (2003), pp. 2280–2299.
[23] N. Wagner, I. Balberg, and D. Klein, *Monte Carlo results for continuum percolation in low and high dimensions*, Phys. Rev. E 74(1) (2006), p. 011127.
[24] E.J. Garboczi, K.A. Snyder, J.F. Douglas, and M.F. Thorpe, *Geometrical percolation-threshold of overlapping ellipsoids*, Phys. Rev. E 52(1) (1995), pp. 819–828.
[25] C.Y. Li and T.W. Chou, *Continuum percolation of nanocomposites with fillers of arbitrary shapes*, Appl. Phys. Lett. 90(17) (2007), p. 174108.
[26] S. Yashonath and P. Santikary, *Influence of non-geometrical factors on intracrystalline diffusion role of sorbate zeolite interactions*, Mol. Phys. 78(1) (1993), pp. 1–6.
[27] G. Arya, E.J. Maginn, and H.C. Chang, *Effect of the surface energy barrier on sorbate diffusion in AlPO4-5*, J. Phys. Chem. B 105(14) (2001), pp. 2725–2735.
[28] S. Srebnik, I. Yungerman, G. Kochav, and M. Sheintuch, *Activated diffusion in relaxed porous structures*, Chem. Eng. Sci. 62 (2007), pp. 2242–2253.
[29] S.K. Bhatia, *Influence of adsorbate interaction on transport in confined spaces*, Adsorp. Sci. Technol. 24(2) (2006), pp. 101–116.
[30] P. Meakin, *Diffusion-limited aggregation in 3 dimensions – results from a new cluster cluster aggregation model*, J. Colloid Interface Sci. 102(2) (1984), pp. 491–504.
[31] D. Dubbeldam, E. Beerdsen, S. Calero, and B. Smit, *Molecular path control in zeolite membranes*, Proc. Natl Acad. Sci. USA 102(35) (2005), pp. 12317–12320.
[32] D. Dubbeldam, E. Beerdsen, S. Calero, and B. Smit, *Dynamically corrected transition state theory calculations of self-diffusion in anisotropic nanoporous materials*, J. Phys. Chem. B 110(7) (2006), pp. 3164–3172.
[33] S.K. Bhatia and D. Nicholson, *Anomalous transport in molecularly confined spaces*, J. Chem. Phys. 127(12) (2007), p. 11.
[34] S. Condamin, O. Benichou, V. Tejedor, R. Voituriez, and J. Klafter, *First-passage times in complex scale-invariant media*, Nature 450(7166) (2007), pp. 77–80.
[35] B.J. Sung and A. Yethiraj, *The effect of matrix structure on the diffusion of fluids in porous media*, J. Chem. Phys. 128 (2008), p. 054702.
[36] C. Loverdo, O. Benichou, M. Moreau, and R. Voituriez, *Enhanced reaction kinetics in biological cells*, Nat. Phys. 4 (2008), pp. 134–137.
[37] L.P. Xue, O. Borodin, and G.D. Smith, *Modeling of enhanced penetrant diffusion in nanoparticle-polymer composite membranes*, J. Membrane Sci. 286(1–2) (2006), pp. 293–300.
[38] T. Elias-Kohav, M. Sheintuch, and D. Avnir, *Steady-state diffusion and reactions in catalytic fractal porous-media*, Chem. Eng. Sci. 46(11) (1991), pp. 2787–2798.